

New Insights into Cutaneous Laser Stimulation – Dependency on Skin and Laser Type

Frahm, Ken Steffen; Gervasio, Sabata; Arguissain, Federico; Mouraux, André

Published in:
Neuroscience

DOI (link to publication from Publisher):
[10.1016/j.neuroscience.2020.09.021](https://doi.org/10.1016/j.neuroscience.2020.09.021)

Creative Commons License
CC BY-NC-ND 4.0

Publication date:
2020

Document Version
Accepted author manuscript, peer reviewed version

[Link to publication from Aalborg University](#)

Citation for published version (APA):
Frahm, K. S., Gervasio, S., Arguissain, F., & Mouraux, A. (2020). New Insights into Cutaneous Laser Stimulation – Dependency on Skin and Laser Type. *Neuroscience*, 448, 71-84.
<https://doi.org/10.1016/j.neuroscience.2020.09.021>

General rights

Copyright and moral rights for the publications made accessible in the public portal are retained by the authors and/or other copyright owners and it is a condition of accessing publications that users recognise and abide by the legal requirements associated with these rights.

- Users may download and print one copy of any publication from the public portal for the purpose of private study or research.
- You may not further distribute the material or use it for any profit-making activity or commercial gain
- You may freely distribute the URL identifying the publication in the public portal -

Take down policy

If you believe that this document breaches copyright please contact us at vbn@aub.aau.dk providing details, and we will remove access to the work immediately and investigate your claim.

Neuroscience

New insights into cutaneous laser stimulation – dependency on skin and laser type --Manuscript Draft--

Manuscript Number:	NSC-20-0825R2
Article Type:	Research Paper
Section/Category:	Pain and Sensory Neuroscience
Keywords:	Pain research; Laser stimulation; computational modeling; model validation; CO ₂ laser; Nd:YAP laser
Corresponding Author:	Steffen Frahm, PhD, MSc BME Aalborg Universitet Aalborg, DK DENMARK
First Author:	Ken Steffen Frahm, PhD, MSc BME
Order of Authors:	Ken Steffen Frahm, PhD, MSc BME Sabata Gervasio, PhD Federico Arguissain, PhD André Mouraux, MD, PhD
Abstract:	<p>Cutaneous laser stimulation is a proficient tool to investigate the function of the nociceptive system. However, variations in laser-skin interactions, caused by different skin anatomies and laser wavelength, affects the robustness of nociceptor activation. Thus, thoroughly understanding how the skin is heated by a laser pulse is important to characterize the thermal response properties of nociceptors. The study aim was to investigate how skin type and laser wavelength influences nociceptor activation during laser stimulation. Ten healthy subjects were exposed to brief CO₂ (low skin penetrance) and Nd:YAP (high skin penetrance) laser stimuli delivered to the dorsum and palm of the hand, using three different intensities. Reaction times and perception intensities were recorded. A computational model simulated heat transfer in the skin and nociceptor activation in different skin types across different wavelengths and intensities. Intensity ratings were significantly lower and reaction-times significantly increased for CO₂ laser stimuli in the palm compared to the dorsum. This was not the case for Nd:YAP laser stimuli. The computational model showed that these differences can be explained by the different skin absorption of CO₂ and Nd:YAP lasers. For CO₂ laser stimuli, the thicker stratum corneum of the glabrous skin reduces nociceptor activation, whereas the high penetrating Nd:YAP laser elicits a similar nociceptor activation, irrespective of skin type. Nociceptor activation during laser stimulation highly depends on skin composition and laser wavelength, especially for lasers having a low penetrance wavelength. A computational model showed that this difference could be primarily due to differences in skin composition.</p>

Title:

New insights into cutaneous laser stimulation – dependency on skin and laser type

Authors: Ken Steffen Frahm ¹, Sabata Gervasio ², Federico Arguissain ¹, André Mouraux ³

¹ Integrative Neuroscience group, CNAP – Center for Neuroplasticity and Pain, SMI[®],

Dept. of Health Science & Technology, Aalborg University, Denmark

² Neural Engineering and Neurophysiology group, SMI[®], Dept. of Health Science & Technology, Aalborg University, Denmark

³ Université Catholique de Louvain, Institute of Neuroscience (IoNS), Faculty of Medicine, Bruxelles, Belgium

Corresponding author:

K.S. Frahm – ksf@hst.aau.dk

Introduction

The study of nociceptive processing and pain perception in humans relies heavily on methods that can selectively activate nociceptors. Over the past 30 years, several studies have employed laser stimulation to selectively activate heat-sensitive A δ - and C-fiber nociceptors in the superficial layers of the skin (Arendt-Nielsen and Chen, 2003; Plaghki and Mouraux, 2005).

How much a given laser pulse applied onto the skin will activate nociceptors is strongly dependent on how that laser pulse will heat the skin at the depth where nociceptive free nerve endings are located (Cruccu et al., 2008). For this reason, the responses triggered by a laser stimulus are strongly dependent on the wavelength of the laser and the pigmentation of the skin (which affect how the laser radiation is transferred to the skin) (Plaghki and Mouraux, 2003), as well as skin thickness (which determines the depth at which nociceptors are located) and laser pulse characteristics such as stimulus duration, beam diameter, and power output.

The complex interactions between laser wavelength, laser pulse parameters and skin characteristics are not thoroughly understood. Studies in the mid-90s suggested a clear difference between how a CO₂ laser heat pulse (wavelength: 10,600 nm) activates nociceptive free nerve endings in hairy and glabrous skin (Treede et al., 1995). That difference was first interpreted as evidence for an apparent lack of quickly-responding heat- and mechano-sensitive Type II A-fibre nociceptors (AMH-2) in the glabrous skin. This interpretation was further used to explain why it was not possible to elicit so-called 'first pain' in glabrous skin when using CO₂ laser stimuli (Campbell and LaMotte, 1983). However, more recent evidence cast doubt on this interpretation (Iannetti et al., 2006). Particularly, Iannetti et al. (2006) applied laser pulses onto the glabrous skin of the hand palms using an Nd:YAP laser (wavelength: 1,340 nm) and found that such stimuli were actually able to elicit responses compatible with the activation of AMH-2 nociceptors. The authors hypothesized that this contrasting observation was due to the skin being more transparent to the Nd:YAP laser wavelength as compared to the CO₂ laser wavelength. The greater transparency of the skin would allow the thermal energy of the Nd:YAP laser to be deposited adjacent to the nociceptors located underneath the thick corneous layer of glabrous skin, rather than being absorbed in the most superficial layers of the skin as done by CO₂ lasers and contact thermodes. This explanation is also supported by recent evidence that showed that the threshold for first pain elicited by a contact thermode was significant higher in the glabrous skin as compared to the hairy skin (Eckert et al., 2017). In addition, other studies have demonstrated differences in the latencies of laser-evoked brain potentials (LEPs) elicited by CO₂ and Nd:YAP laser pulses applied onto the hairy skin (Cruccu et al., 2008), as well as between the latencies of LEPs and contact heat-evoked potentials (CHEPs) (Iannetti et al., 2006). These latency differences could be explained by the fact that if a thermal stimulus only

heats the most superficial layers of the skin, it requires a certain amount of time for the heat to be transferred into the deeper skin layers. Taken together, it can be speculated that heat transduction in the skin probably differs significantly across laser types. Still, evidence that confirms these findings is lacking. Moreover, it remains largely unknown how laser pulse parameters such as stimulus duration and power affects heat transduction and thus the ability of the stimulus to activate nociceptors. In this regard, computational modeling provides a tool to predict heat transduction in the skin (Frahm et al., 2010; Marchandise et al., 2014; Mørch et al., 2015). Combined with psychophysics and other means to assess whether and how a given stimulus activates nociceptors, such models could provide insights into the heat transduction, but also describe where and when the tissue temperature reaches the threshold for activating nociceptive afferents.

The aim of this study was to provide a better understanding of how nociceptors of the hairy skin and glabrous skin are activated during stimulation with two different laser wavelengths. Using a combined experimental and computational approach, the second aim of the study was to develop and validate a new computational model to investigate the characteristics of both lasers and skin types, such as laser absorption profiles and skin composition.

To validate the model for the laser stimulation, the temporal and spatial temperature profiles were compared across two laser types (CO₂ vs. Nd:YAP), skin type (glabrous vs. hairy) and stimulation intensity. This information was then combined with a series of psychophysical measures, allowing further investigation of differences in activation of heat-sensitive nociceptors across skin types, laser types and stimulation intensity.

Experimental Procedures

Experimental setup

Subjects

Ten healthy subjects participated in this study (average age: 29±4 years, five females). All subjects were Caucasian with clear skin. During the experiment, the subjects were placed in a bed with the headrest raised for comfort. Prior to the experiment, both oral and written consent was obtained from the subjects. The Declaration of Helsinki was respected. The experiment was approved by the local ethical committee (N-20140093).

Laser stimulation

Each subject was stimulated with two types of lasers (CO₂ – 10,600 nm and Nd:YAP 1,340 nm) at both the dorsum and the palm of the right hand. Subjects received laser stimuli at three different intensities. For each type of laser, the intensities were chosen based on pilot experiments performed at the dorsum of the hand.

To ensure similarity, these pilot experiments were conducted using the same number of stimuli repetitions as in the final study (see below). The stimulus intensities were adjusted so that they were perceived equally intense for the Nd:YAP and CO₂ lasers. Particularly, the stimulus intensities were adjusted at the hand dorsum for both lasers so that the lower intensity was below pain threshold, the medium intensity was close to pain threshold, and the high intensity was above pain threshold. Due to the different penetration profiles of the two lasers, the stimulation duration was 200 ms for the CO₂ laser and 20 ms for the Nd:YAP laser. As compared to what is often used during laser stimuli (typically between 4 and 20 ms for Nd:YAP LEPs and between 15 and 200 ms for CO₂ LEPs (Bromm et al., 1984; Moore and Schady, 1995; Arendt-Nielsen and Chen, 2003; Truini et al., 2005; Perchet et al., 2008)), the chosen stimulus durations were relatively long. This decision was made to obtain enough infrared imaging time points to validate the computational model.

For each of the three intensities, the power settings of the CO₂ laser were 3.7, 4.8 and 5.6 W (the respective energies were 0.74, 0.96 and 1.12 J), and the power settings for the Nd:YAP laser were 175, 200 and 225 W (the energies were 3.5, 4.0 and 4.5 J). The diameter of the laser beam was 5.7 mm for the CO₂ laser (1/e², gaussian distribution) and 4 mm (1/e², gaussian distribution) for the Nd:YAP laser. During the experiment both the subject and investigators wore protective goggles.

Experimental protocol

The experiment consisted of a single session lasting approximately 1.5 hours. All combinations of laser type (CO₂ and Nd:YAP), stimulation intensity (low, medium, high) and skin type (dorsum and palm) were randomized. A total of 5 stimuli was given consecutively for each combination. The inter-stimulus interval was randomized between 15 and 45 seconds, and the stimulus site was changed between each stimulus. Following each stimulation, subjects had to push a button as soon as any stimulation was felt, in order to estimate their reaction times. Then, the subjects were asked to rate their perceived intensity on a Numerical Rating Scale (NRS) anchored as 0: perception threshold, 3: pain threshold, 10: maximum pain. Additionally, after each stimulus combination, the subjects were asked to rate the perceived quality of the stimulation using the short-form McGill Pain Questionnaire (SF-MPQ) (Melzack, 1987).

Infrared (IR) thermography of the skin surface was recorded during laser stimulation (Agema 900, FLiR, Sweden – Frame-rate 30Hz). These data were further used to validate the computational model.

Computational modeling of cutaneous laser stimulation

The computational model in this study is based on the Finite Element Method. The model was developed and computed using COMSOL Multiphysics 5.4 (COMSOL A/S, Stockholm, Sweden). The model was implemented using a 2D-axial symmetrical geometry (Figure 1). To simulate anatomical differences between

the hairy skin in dorsum of the hand and the glabrous skin in palm of the hand, the thickness of the stratum corneum and vital epidermis were varied to account for the thicker epidermal layers of glabrous hand skin as compared to hairy hand skin (Figure 1). The depth of the dermo-epidermal junction (DEJ) was set to 130 μm for glabrous skin and 50 μm for hairy skin. The width of the model was 5 cm, and it was determined based on a convergence analysis, ensuring that the simulation of the temperature had converged at this model width. The absorption of the laser photons was based on the Beer-Lambert's equation similar to previous studies (Frahm et al., 2010; Marchandise et al., 2014), and the beam profiles of the two lasers were both modelled as Gaussian (Eq. 1). Therefore, the laser heating, Q , becomes:

$$Q(\mathbf{r}, t) = P_{in} \mu_a e^{(-\mu_a z)} \frac{1}{\sigma \sqrt{2\pi}} e^{\left(\frac{-r^2}{2\sigma^2}\right)} \quad (1)$$

Where \mathbf{r} is the spatial coordinate (consisting of the radial coordinate r and the depth coordinate z), t is time, P_{in} is the laser power, μ_a is the absorption coefficient and σ is the radius of the laser beam ($1/e^2$, gaussian distribution).

[Insert Fig. 1]

The optical and thermal parameters were based on the literature and fitted with the experimental data to ensure optimal coherence (Figure 1). The obtained optical parameters were laser wavelength dependent, but the thermal parameters were not. Therefore, the optical parameters (absorption coefficient, μ_a) were adjusted for each type of laser. For the Nd:YAP laser wavelength (1,340 nm), the optical parameters were based on (Salomatina et al., 2006; Frahm et al., 2010; Jacques, 2013; Marchandise et al., 2014; Nasouri et al., 2014). For wavelengths far above 1,100 nm, the optical parameters of the tissue approach those of water (Bromm and Treede, 1983; Friebel et al., 2009), which also includes the CO₂ laser wavelength (10,600nm). Since the water content is lower in the stratum corneum and epidermis than in the dermis (Marchandise et al., 2014), the absorption coefficient is therefore lower in the more superficial tissues. With this in mind, the optical parameters for the CO₂ laser were based on (Frahm et al., 2010; Jacques, 2013; Marchandise et al., 2014).

The thermal parameters (thermal conductivity, k ; specific heat, c ; and density, ρ) were identical for both laser types. The lower water content of the superficial tissues, i.e. stratum corneum and epidermis, results in lower specific heat and thermal conductivities than in the deeper dermis. The thermal parameters were based on (Wilson and Spence, 1988; Frahm et al., 2010; Marchandise et al., 2014).

The heat generation and transport within the tissue was modelled using the bio-heat equation (Eq. 2):

$$\rho c \frac{\partial T(\mathbf{r}, t)}{\partial t} - \nabla \cdot (k \nabla T(\mathbf{r}, t)) = Q(\mathbf{r}, t) \quad (2)$$

The thermal parameters, k , ρ and c , can be seen in Figure 1. Based on the IR recordings, the initial tissue temperature in the model was set to 35 °C, and the lower boundary was fixed at 35 °C to simulate the heat sink through blood vessels in the lower dermis (Frahm et al., 2010).

The meshed model consisted of 20639 mesh elements for the dorsum model and 15182 mesh elements for the palm model. The solution time was approx. 5 minutes on a standard computer (Intel i7-6600u, 20 GB RAM).

Data analysis & statistics

Experimental data

The spatial and temporal temperature profiles at the skin surface were extracted from the IR recordings to validate the computational model. The temporal profiles were extracted as the maximum skin temperature during baseline, stimulation and subsequent cooling phase. The temporal profiles were extracted from one second before stimulus onset, to five seconds after stimulus offset. The spatial profile was extracted at stimulus end. To obtain a spatial reference in the IR recordings, a 10x10 mm aluminum plate was placed within the IR camera frame. It was further ensured that the plate was oriented in the same plane as the stimulation site (Frahm et al., 2010). The two pixels vectors, corresponding to the diagonals of the aluminum plate, were moved to the stimulation location of the IR frame to extract the spatial temperature profile.

Once the data were extracted, the 95 % confidence interval (CI) was calculated for all stimulus conditions. The 95 % CI was compared with the predicted profiles from the computational model, in a similar fashion to the validation method used in (Frahm et al., 2010).

The psychophysical measures (reaction time, NRS and SF-MPQ) were analyzed using three separate three-way repeated-measures analyses of variance (RM-ANOVAs) with the factors laser wavelength (two levels: Nd:YAP, CO₂), stimulus intensity (low, medium, high) and skin type (glabrous, hairy). The Shapiro-Wilk test (together with skewness and kurtosis of the distributions) was adopted to check for normality of the data. All data was normally distributed. Mauchly's test of sphericity was adopted to check for equal variances. Since data for the RT and McGill questionnaire were not spherical, Greenhouse-Geisser correction was adopted in these cases.

Model data

The model was validated by comparing the predicted temperature profiles (temporal and spatial) to the 95% CI from the experimental IR data.

After model validation, the simulated temperature profiles within the tissue were extracted to investigate the possible differences across laser wavelengths, skin type and stimulation intensity. Furthermore, the model was used to extract the total area above nociceptor threshold for different depths within the vital tissues. This was done by integrating the area across the entire model width for each depth, in steps of 1 μm . The thermal threshold for C-fibers was set to 41 $^{\circ}\text{C}$, and the thermal threshold A δ fibers was set to 46 $^{\circ}\text{C}$. These thresholds were chosen based on the results of previous studies indicating that, for short-lasting CO₂ laser pulses delivered onto the hairy skin, the surface temperature threshold is approximately 41 $^{\circ}\text{C}$ for C-fiber input and 46 $^{\circ}\text{C}$ for A δ -fiber input. The model was also used to calculate the tissue volume above nociceptor threshold over time. Since heat sensitive nociceptors are located within the basal and spinous layers of the epidermis and the upper part of the dermis, the tissue volumes were calculated for this part of the model.

Finally, the maximum tissue volumes for each laser wavelength, skin type and intensity were compared to the according psycho-physical findings (NRS). This comparison was made using a Pearson's linear correlation analysis between the maximum activated volume for both C and A δ fibers vs. the reported NRS from the subjects.

Results

Experimental results

The reported NRS showed a significant interaction between skin and laser type (RM-ANOVA, $F_{1,9}=19.42$, $p<0.01$, $\eta_p^2=0.68$). Particularly, subjects reported significantly lower NRS scores when stimulating the palm of the hand with the CO₂ laser (Figure 2) Moreover, subjects reported significantly higher NRS scores for higher stimulation intensities regardless of laser type (Figure 2; RM-ANOVA, $F_{2,18}=115.20$, $p<0.001$, $\eta_p^2=0.93$).

[Insert Fig. 2]

The reported reaction times showed a significant interaction between skin and laser type (Figure 3, RM-ANOVA, $F_{1,9}=18.71$, $p<0.001$, $\eta_p^2=0.68$). The average reaction times to CO₂ laser stimuli delivered onto the palm were significantly longer. There was also a significant main effect of laser type (RM-ANOVA, $F_{1,9}=8.53$, $p<0.05$, $\eta_p^2=0.49$), skin type (RM-ANOVA, $F_{1,9}=5.86$, $p<0.05$, $\eta_p^2=0.39$), and stimulation intensity (RM-ANOVA, $F_{2,18}=43.81$, $p<0.001$, $\eta_p^2=0.83$). The reaction times decreased with increasing stimulation intensities.

Because of the slower conduction velocity of unmyelinated C fibers, reaction times to stimuli delivered at the distal end of a limb can be used to distinguish responses conveyed by A δ and C fibers. Although interindividual differences in peripheral conduction distance can be expected to produce interindividual differences in reaction times, previous studies using brief CO₂ laser pulses have shown that a 650 ms cutoff effectively separates A- and C-fiber mediated detections for stimuli delivered to the hand dorsum (Mouraux et al., 2003; Jankovski et al., 2013). Other factors such as heating velocity at the stimulation site, which can differ between skin and laser types, may also influence reaction times. Nevertheless, comparing the reaction times to a 650 ms cut-off to separate responses to nociceptive input conveyed by thinly-myelinated A δ -fibers vs. unmyelinated C-fibers, most of the high intensity stimuli delivered to the hand dorsum could be considered as being related to A δ fiber activation regardless of laser type. In contrast, when the same high-intensity laser stimuli were delivered to the hand palm, Nd:YAP laser stimuli were detected with reaction times indicating A δ fiber activation, whereas CO₂ laser stimuli were most-often detected with reaction-times indicating C-fiber mediated detections (Figure 3).

[Insert Fig. 3]

The responses to the SF-MPQ showed a significant interaction between laser and skin type (Figures 4 & 5, RM-ANOVA, $F_{1,9} = 10.24$, $p < 0.05$, $\eta_p^2 = 0.53$) and between stimulation intensity and skin type (Figures 4 & 5, RM-ANOVA, $F_{2,18} = 9.03$, $p < 0.01$, $\eta_p^2 = 0.50$). There were significant main effects of skin type ($F_{1,9} = 9.05$, $p < 0.05$, $\eta_p^2 = 0.50$), laser type ($F_{1,9} = 11.90$, $p < 0.01$, $\eta_p^2 = 0.57$), stimulation intensity ($F_{2,18} = 17.01$, $p < 0.01$, $\eta_p^2 = 0.65$) and pain descriptor ($F_{14,126} = 44.00$, $p < 0.001$, $\eta_p^2 = 0.83$). The descriptors 'Sharp' and 'Hot-burning' were used more often than all other descriptors (pairwise multiple comparisons, all $p < 0.001$).

[Insert Fig. 4 & 5]

Simulation results

The model parameters could be fitted so that there was agreement between the model and the experimental infrared imaging data for all combinations of skin type, laser wavelength and stimulation intensity (Figures 6 & 7).

[Insert Fig. 6 & 7]

Comparing the simulated temperatures at the skin surface and the dermo-epidermal junction (DEJ), it is evident that there was little difference in temperature between the skin surface and the DEJ for the Nd:YAP stimuli, whereas there was a larger temperature difference between the skin surface and the DEJ for CO₂ stimuli (Figure 8). Expectedly, this latter difference was increased for stimuli delivered to the glabrous skin of the palm. In the most extreme case, the difference was more than 10 °C. When these differences are

quantified, it becomes evident that the surface temperature in the glabrous skin is highest for CO₂ laser stimuli, but the DEJ temperature is lowest for these stimuli (Figure 9). It is interesting that this tendency was reversed for the Nd:YAP laser, where the delay to reach maximum DEJ temperature in the dorsum was longer than it was in the palm (Figure 9).

[Insert Fig. 8]

[Insert Fig. 9]

The difference between the Nd:YAP and CO₂ lasers becomes even more evident when using the model to investigate the potential nociceptor activation throughout the tissue (Figure 10). It is clear that the CO₂ laser pulses create a spatially widespread, but very superficial activation volume. In contrast, the Nd:YAP laser creates a spatially more focused but much deeper activation volume that extends far beyond the epidermis (50 µm in the dorsum; 130 µm in the palm – vertical grey lines in Figure 10) and into most of the dermis. In fact, the activation is so deep that C-fibers may be activated at a depth of more than 1 mm, i.e. inside the deep dermis. Figure 10 also shows that the high-intensity CO₂ stimuli delivered to the hand palm may not activate any Aδ nociceptors at the DEJ.

[Insert Fig. 10]

The simulation of the tissue volume above thermal activation threshold (Figure 11) showed that for the low stimulation intensity, the model predicted that only C- and no Aδ-fiber activation could occur. Unsurprisingly, the tissue volume where C-fiber activation could occur was always larger than the volume for Aδ-fiber activation, due to the lower thermal threshold of C-fibers. With higher stimulation intensities, the volume above threshold increases, and it becomes possible to activate Aδ fibers (Figure 11; Medium & High intensity). Again, it is worth noting the contrasting findings for CO₂ laser stimuli in the palm compared to the other combinations of laser and skin types, which showed that CO₂ laser stimuli in the palm activated a smaller volume of nociceptors for both C and Aδ fiber nociceptors.

[Insert Fig. 11]

Experimental vs. computational results

There was a significant correlation (Pearson, $p < 0.0001$, $r > 0.9$) between the maximum simulated tissue volumes above nociceptor threshold (from Figure 11) and the experimentally found NRS for both the C- and Aδ fiber simulation (Figure 12). This suggests that the computational model can indeed predict the experimental results.

[Insert Fig. 12]

Discussion

This study investigated how the activation of heat-sensitive nociceptors by laser heat stimuli depends on laser wavelength and skin type (dorsum and palm of the hand). A computational model was developed and validated to further investigate and explain these differences. Our results showed a clear difference in how cutaneous laser stimulation activates nociceptive afferents, depending on the combination of laser wavelength and skin type. Especially, we confirm that CO₂ laser stimuli in the glabrous skin of the palm cause a significant lower degree of nociceptor activation compared to the same stimuli delivered to hairy skin, or to Nd:YAP laser stimuli delivered to glabrous skin. Our simulations show that this can be explained entirely by differences in skin composition and thickness.

Cutaneous nociceptor activation following laser stimuli

In this study, the subjects were stimulated with three different intensities that were below, above and close to pain threshold (Figure 2). Thus, this study gives insights to various levels of nociceptor activation. The perceived intensities, perception qualities and reaction times were similar for both Nd:YAP and CO₂ laser stimuli delivered to the dorsum of the hand. Increased stimulation intensity caused increased perceived intensities (Figure 2), shorter reaction times (Figure 3) and higher usage of the 'Sharp' descriptor on the SF-MPQ (Figures 4 & 5). A possible reason for this might be that higher intensities are more likely to activate A δ fibers which have a higher conduction velocity than C fibers, resulting in shorter average reaction times.

Activation of A δ fibers is also expected to increase the usage of the 'Sharp' descriptor, which is typical quality of 'first pain' (Hansen et al., 2007). On the other hand, the 'Hot/burning' descriptor is believed to be associated with activation of C fibers (Mackenzie et al., 1975; Magerl et al., 1999; Hansen et al., 2007). Additionally, higher stimulation intensities cause a larger tissue volume to be above thermal threshold (Figure 11), creating an increased afferent signal to the central nervous system, which might also lead to an increased perception intensity and changes in perception quality.

At first, the similar psychophysical ratings from the dorsum could indicate that the neural activation from both laser types are very similar within this region, and thus it does not depend on the laser wavelength. However, the insights from the model suggest that these two lasers may activate different subgroups of afferents (Figure 10). The Nd:YAP laser appears to be capable of activating nociceptors in the deeper parts of the epidermis and most of the dermis, whereas CO₂ laser stimuli appear only to be able to activate intra-epidermal nociceptors. In the glabrous skin, only epidermal nociceptors that terminate extremely close to the surface may be activated with the CO₂ laser, if any. Since the highest density of nociceptors appears to be around the DEJ (Frahm et al., 2010), this could explain the lower intensity ratings for CO₂ laser stimuli

delivered to the palm, as the majority of the nociceptors may not be activated. Additionally, because of the greater spatial spread of the temperature increase produced by Nd:YAP laser stimuli, these may also be expected to activate a greater number of heat-sensitive free nerve endings having a low thermal activation threshold, such as warm-sensitive C-fibers. This co-activation could affect the elicited responses, especially when investigating heat-evoked C-fiber responses.

When comparing the size of the tissue volume above nociceptor threshold, it becomes evident that the CO₂ laser activates a slightly larger volume than the equivalent Nd:YAP laser. However, the tissue is above threshold for a longer period for the Nd:YAP laser (Figure 11), in some cases more than one second. This is the case even when the Nd:YAP laser has a shorter stimulation duration (20 ms). The reason for this appears to be that the thermal energy 'lingers' in the tissue, due to larger penetration of the Nd:YAP laser, which creates a smaller temperature gradient in tissue (Eq. 2) prolonging the cooling phase – a notion which is supported by the infrared recordings of skin surface temperature Figure 6 & 7). This prolonged period above activation threshold may cause after-sensations or prolonged neural activation for this laser type. This may explain why the psychophysical ratings are still similar for Nd:YAP and CO₂ laser stimuli delivered to the hand dorsum, but could also indicate fundamental differences between laser types, which would need further investigation. In this regard, the high penetration of the Nd:YAP could also explain why C-fiber mediated LEP responses appear to be easier to elicit using Nd:YAP laser stimuli (Hu et al., 2014; Jin et al., 2018), compared to CO₂ laser stimuli (Figure 10). Nevertheless, it is interesting to see the strong correlation between the simulated tissue volumes and intensity ratings (Figure 12), which indicates that the maximum tissue volume above the thermal threshold is most useful for predicting perceived intensity. This high correlation between computational and experimental data further underlines the validity of the model. The main difference between hairy and glabrous skin appears to be the thickness of the tissue layers, rather than differences in neural populations or their density.

The lack of A δ fiber activation during CO₂ stimulation of the palm does not appear to be due to lack of AMH-2 in the glabrous skin as suggested by (Treede et al., 1995). Instead, the present results suggest that CO₂ laser stimulation in the palm does not entail a sufficient temperature increase where A δ -fiber free nerve endings are located. This is further supported by the fact Nd:YAP stimuli to the palm caused perceptions that appear to be mediated by nociceptors with similar response properties of AMH-2. This is in agreement with another study that compared contact-heat and Nd:YAP laser stimuli in both hairy and glabrous skin and found similar responses when using the high-penetrating Nd:YAP laser (Iannetti et al., 2006).

Modeling cutaneous laser stimulation

The current model uses a similar approach as seen in other studies that used computational modeling to investigate cutaneous laser stimulation (Bromm and Treede, 1983; Frahm et al., 2010; Marchandise et al., 2014). However, most previous studies that applied computational modeling of cutaneous heat stimulation either did not validate the model or they validated them against previous models that were developed to investigate a different problem. Both approaches constitute major limitations that questions the results and interpretations obtained from such models. To circumvent this lack of proper validation, this study used the infrared measurements of the skin surface temperature to validate the model. The infrared measurements were used because such measurements will not affect the thermodynamics of the skin. In contrast, small intra-cutaneous probes will always affect the thermal system – and the exact location of the probes may be unknown or slightly imprecise (Bromm and Treede, 1983), making the recordings less reliable. The present results showed that the current model had good agreement with the experimental data. The fact that the model shows good agreement across both two different wavelengths, two different tissue geometries and three stimulation intensities is a strong argument for the validity of the present model.

Since the thermal thresholds of C- and A δ -fiber nociceptors for surface temperature are estimated to be approx. 41 and 46 °C, respectively (Treede et al., 1995; Churyukanov et al., 2012), these temperature profiles were extracted from the model and compared with the psychophysical results. The surface temperature may, however, not be identical to the actual thermal threshold within the tissue, but no such data exist. The overall finding from the model is that skin thickness appears to explain the experimental differences between different skin types. Additionally, the model shows that different laser types (wavelength) may cause different nociceptor activation. The high penetration Nd:YAP laser appears to be able to mitigate the differences in nociceptors between skin types for the CO₂ laser. This is most likely because the Nd:YAP deposits the thermal energy deeper than the CO₂ laser – a finding which is supported by both the experimental data and model.

Temperature at the skin surface does not correlate with nociceptor activation

One of the skin's primary functions is to reduce the bodily heat loss to the surroundings; therefore, the outer-most skin layers have very low thermal conductivity (Wilson and Spence, 1988). This is important, because within the outer-most layer of the skin, the stratum corneum, no nociceptors or other receptor types are found. Instead, the receptors terminate in the dermis and within the basal and spinous layers of the epidermis (Ebenezer et al., 2007). This means that any thermal stimulus applied to the skin surface has to be passively conducted into the deeper layers to activate the receptors, whereas high penetrance laser stimuli such as Nd:YAP stimuli, may irradiate the receptors directly. The depth of the receptors depends on the skin

1 type and particularly the thickness of the stratum corneum – thicker skin means deeper receptor location
2 (Frahm et al., 2010).
3

4
5 Previous studies have shown how the thermal threshold of these nociceptors may depend on the initial skin
6 temperature (Pertovaara et al., 1996; Churyukanov et al., 2012). However, it is important to notice that all
7 these studies either used contact-heat stimuli or CO₂ laser stimuli, to both change the initial temperature and
8 activate the nociceptors. Yet, there is a clear discrepancy between skin surface temperature and the
9 nociceptor temperature when using these stimulation methods (Figure 8). In this context, it is also interesting
10 that the highest skin surface temperatures were observed for CO₂ laser stimuli delivered to the palm (Figures
11 6 & 7), even though this combination appears to exhibit the lowest DEJ temperature (Figures 8 & 9) and the
12 lowest intensity ratings (Figure 2). This phenomenon is most likely caused by thicker stratum corneum and
13 vital epidermis in glabrous skin that prevent the heat to reach the receptors, due to a thicker tissue layer with
14 low thermal conductivity. This finding also explains why studies have shown that the heat pain threshold
15 (HPT) is increased with increased stimulation ramps (Tillman et al., 1995), likely reflecting the effect of
16 thermal inertia of the skin. The HPT has been reported to be 43-46 °C for stimulation ramps of 2 °C/s
17 (Yarnitsky et al., 1995; Defrin et al., 2002), but it can exceed 50 °C for higher ramps (10 °C/s) (Pertovaara et
18 al., 1996). Higher ramps would increase skin surface temperature faster, but the receptor temperature would
19 not increase at the same rate. Thus, the findings in this study indicate that the higher HPT for higher ramps
20 may have little to do with the neural function of the thermoreceptive afferents in skin, but merely be a
21 consequence of the low thermal conductivity of the superficial skin layers. It should also be noted that the
22 photons from a CO₂ laser does penetrate slightly, but not deep enough to be absorbed directly at the location
23 of the receptors.
24
25

26
27 During cutaneous thermal stimuli, one would assume that the skin surface temperature is higher than deeper
28 in the skin. This is indeed the case for CO₂ lasers and contact heat probes; however, this is not the case for
29 Nd:YAP lasers. In fact, during Nd:YAP stimuli, the DEJ temperature is initially higher than the skin surface
30 temperature (Figure 8) and the delay to reach the maximum skin surface temperature is much longer than
31 stimulus duration (Figure 9). This phenomenon is most likely cause by the high penetration of the Nd:YAP
32 laser, causing the thermal energy to be deposited deep in the skin. The thermal energy is then passively
33 conducted throughout the tissue, including towards the skin surface, causing the maximum skin surface
34 temperature to be reached almost 200 ms after stimulus offset in hairy skin, and more than 400 ms after
35 stimulus offset in glabrous skin (Figure 9).
36
37

38
39 The absorption properties of the Nd:YAP and CO₂ lasers, highly depends on the skin pigmentation (Nd:YAP)
40 and water content (CO₂) (Plaghki and Mouraux, 2003; Perchet et al., 2008). Neither of these parameters were
41
42
43
44
45
46
47
48
49
50
51
52
53
54
55
56
57
58
59
60
61
62
63
64
65

1 included in the current study. Increased pigmentation can expected to markedly increase the absorbance of
2 the Nd:YAP laser. This may be relevant to consider in future studies to ensure similar nociceptor activation
3 across all subjects when testing across larger samples sizes.
4
5

6
7 To summarize, CO₂ laser stimuli delivered to the palm of the hand results in significant lower intensity ratings
8 and slower reaction times compared to CO₂ laser stimuli delivered to the hand dorsum, and compared to
9 Nd:YAP laser stimuli delivered to both skin types. This study shows that when CO₂ laser stimuli are delivered
10 to the palm, the thermal energy is deposited too superficially to achieve the same level of nociceptor
11 activation as similar stimuli given to the hand dorsum. Moreover, it shows that the skin cools more rapidly
12 following CO₂ laser stimulation as compared to Nd:YAP laser stimulation. Hence, for a given target
13 temperature at the level of the epidermis, nociceptors may be activated for a much greater duration
14 following Nd:YAP laser stimulation as compared to CO₂ laser stimulation. Finally, both the experimental data
15 and the modeling data lead to the conclusion that the skin surface temperature may not be a very accurate
16 measure for the potential nociceptor activation elicited by a laser stimulus. This is particularly evident for
17 CO₂ laser stimuli in the palm, which causes the overall highest elevation in skin surface temperature, but
18 results in the lowest nociceptor activation.
19
20
21
22
23
24
25
26
27

28 29 30 31 32 33 34 35 36 37 38 39 40 41 42 43 44 45 46 47 48 49 50 51 52 53 54 55 56 57 58 59 60 61 62 63 64 65

Arendt-Nielsen L, Chen ACN (2003) Lasers and other thermal stimulators for activation of skin nociceptors
in humans. *NeurophysiolClin* 33:259–268.

Bromm B, Jahnke MT, Treede RD (1984) Responses of human cutaneous afferents to CO₂ laser stimuli
causing pain. *Exp Brain Res* 55:158–166.

Bromm B, Treede R-D (1983) CO₂ laser radiant heat pulses activate C nociceptors in man. *Pflügers Arch -
Eur J Physiology* 399:155–156

Campbell JN, LaMotte RH (1983) Latency to detection of first pain. *Brain Res* 266:203–208

Churyukanov M, Plaghki L, Legrain V, Mouraux A (2012) Thermal Detection Thresholds of Aδ- and C-Fibre
Afferents Activated by Brief CO₂ Laser Pulses Applied onto the Human Hairy Skin. *PLoS One* 7:1–10.

Cruccu G, Aminoff MJ, Curio G, Guerit JM, Kakigi R, Mauguiere F, Rossini PM, Treede RD, Garcia-Larrea L
(2008) Recommendations for the clinical use of somatosensory-evoked potentials. *ClinNeurophysiol*
119:1705–1719.

Defrin R, Ohry A, Blumen N, Urca G (2002) Sensory determinants of thermal pain. *Brain* 125:501–510

- Ebenezer GJ, Hauer P, Gibbons C, McArthur JC, Polydefkis M (2007) Assessment of epidermal nerve fibers: a new diagnostic and predictive tool for peripheral neuropathies. *JNeuropatholExpNeurol* 66:1059–1073.
- Eckert NR, Vierck CJ, Simon CB, Cruz-Almeida Y, Fillingim RB, Riley JL (2017) Testing assumptions in human pain models: Psychophysical differences between first and second pain. *J Pain* 18:266–273
- Frahm KS, Andersen OK, Arendt-Nielsen L, Mørch CD (2010) Spatial temperature distribution in human hairy and glabrous skin after infrared CO₂ laser radiation. *Biomed Eng Online* 9:69
- Friebel M, Helfmann J, Netz U, Meinke M (2009) Influence of oxygen saturation on the optical scattering properties of human red blood cells in the spectral range 250 to 2000 nm. *J Biomed Opt* 14:034001
- Hansen N, Klein T, Magerl W, Treede RD, Hansen N, Klein T, Magerl W, Treede RD (2007) Psychophysical evidence for long-term potentiation of C-fiber and A-delta-fiber pathways in humans by analysis of pain descriptors. *JNeurophysiol* 97:2559–2563.
- Hu L, Cai MM, Xiao P, Luo F, Iannetti GD (2014) Human Brain Responses to Concomitant Stimulation of A and C Nociceptors. *J Neurosci* 34:11436–11451.
- Iannetti GD, Zambreanu L, Tracey I (2006) Similar nociceptive afferents mediate psychophysical and electrophysiological responses to heat stimulation of glabrous and hairy skin in humans. 1:235–248.
- Jacques SL (2013) Optical properties of biological tissues: a review. *Phys Med Biol* 58:R37–R61
- Jankovski A, Plaghki L, Mouraux A (2013) Reliable EEG responses to the selective activation of C-fibre afferents using a temperature-controlled infrared laser stimulator in conjunction with an adaptive staircase algorithm. *Pain* 154:1578–1587
- Jin QQ, Wu GQ, Peng WW, Xia XL, Hu L, Iannetti GD (2018) Somatotopic Representation of Second Pain in the Primary Somatosensory Cortex of Humans and Rodents. *J Neurosci* 38:5538–5550.
- Mackenzie RA, Burke D, Skuse NF, Lethlean AK (1975) Fibre function and perception during cutaneous nerve block. *JNeurolNeurosurgPsychiatry* 38:865–873.
- Magerl W, Ali Z, Ellrich J, Meyer RA, Treede RD (1999) C- and A-delta-fiber components of heat-evoked cerebral potentials in healthy human subjects. *Pain* 82:127–137.
- Marchandise E, Mouraux A, Plaghki L, Henrotte F (2014) Finite element analysis of thermal laser skin stimulation for a finer characterization of the nociceptive system. *JNeurosciMethods* 223:1–10

- 1 Melzack R (1987) The short-form McGill Pain Questionnaire. *Pain* 30:191–197.
- 2
- 3 Moore CEG, Schady W (1995) Cutaneous localisation of laser induced pain in humans. *Neurosci Lett*
- 4 193:208–210.
- 5
- 6
- 7 Mørch CD, Frahm KS, Coghill RC, Arendt-Nielsen L, Andersen OK (2015) Distinct temporal filtering
- 8 mechanisms are engaged during dynamic increases and decreases of noxious stimulus intensity. *Pain*
- 9 156:1906–1912
- 10
- 11
- 12
- 13 Mouraux A, Guérit JM, Plaghki L (2003) Non-phase locked electroencephalogram (EEG) responses to CO₂
- 14 laser skin stimulations may reflect central interactions between A partial partial differential- and C-
- 15 fibre afferent volleys. *Clin Neurophysiol* 114:710–722.
- 16
- 17
- 18
- 19
- 20 Nasouri B, Murphy TE, Berberoglu H (2014) Simulation of laser propagation through a three-layer human
- 21 skin model in the spectral range from 1000 to 1900 nm. *J Biomed Opt* 19:075003
- 22
- 23
- 24 Perchet C, Godinho F, Mazza S, Frot M, Legrain V, Magnin M, Garcia-larrea L (2008) Clinical
- 25 Neurophysiology Evoked potentials to nociceptive stimuli delivered by CO₂ or Nd : YAP lasers. *Clin*
- 26 Neurophysiol 119:2615–2622
- 27
- 28
- 29
- 30 Pertovaara A, Kauppila T, Hämäläinen MM (1996) Influence of skin temperature on heat pain threshold in
- 31 humans. *Exp Brain Res* 107:497–503
- 32
- 33
- 34 Plaghki L, Mouraux A (2003) How do we selectively activate skin nociceptors with a high power infrared
- 35 laser. Physiology and biophysics of laser stimulation Comment activer selectivement des nocicepteurs
- 36 cutanés avec un laser infrarouge de forte puissance. *Physiologie et biophysiq. Neurophysiol Clin*
- 37 33:269–277.
- 38
- 39
- 40
- 41
- 42 Plaghki L, Mouraux A (2005) EEG and laser stimulation as tools for pain research. *Curr Opin Investig Drugs*
- 43 6:58—64.
- 44
- 45
- 46 Salomatina E, Jiang B, Novak J, Yaroslavsky AN (2006) Optical properties of normal and cancerous human
- 47 skin in the visible and near-infrared spectral range. *J Biomed Opt* 11:064026.
- 48
- 49
- 50
- 51 Tillman DB, Treede RD, Meyer RA, Campbell JN (1995) Response of C fibre nociceptors in the anaesthetized
- 52 monkey to heat stimuli: correlation with pain threshold in humans. *J Physiol* 485 Pt 3:767–774.
- 53
- 54
- 55 Treede RD, Meyer RA, Raja SN, Campbell JN (1995) Evidence for two different heat transduction
- 56 mechanisms in nociceptive primary afferents innervating monkey skin. *J Physiol* 483:747–758
- 57
- 58
- 59
- 60
- 61
- 62
- 63
- 64
- 65

1 Truini A, Galeotti F, Romaniello A, Virtuoso M, Iannetti GD, Cruccu G (2005) Laser-evoked potentials:
2 normative values. Clin Neurophysiol 116:821–826
3

4
5 Wilson SB, Spence VA (1988) A tissue heat transfer model for relating dynamic skin temperature changes to
6 physiological parameters. PhysMedBiol 33:895–912.
7

8
9 Yarnitsky D, Ruth Zaslansley S, Hemji JA (1995) Heat pain thresholds: normative data and repeatability. Pain
10 60:329–332
11
12
13
14
15
16
17
18
19
20
21
22
23
24
25
26
27
28
29
30
31
32
33
34
35
36
37
38
39
40
41
42
43
44
45
46
47
48
49
50
51
52
53
54
55
56
57
58
59
60
61
62
63
64
65

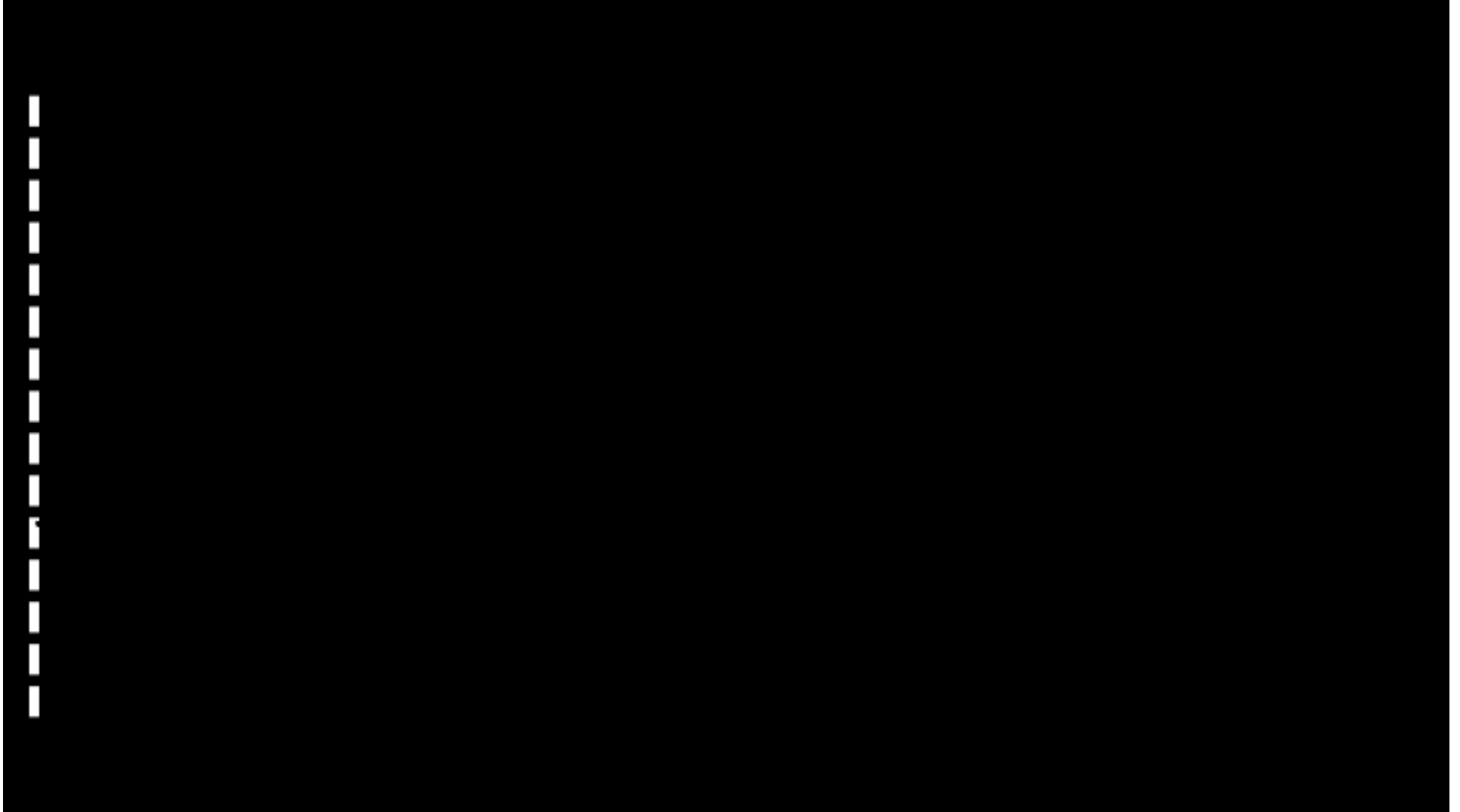
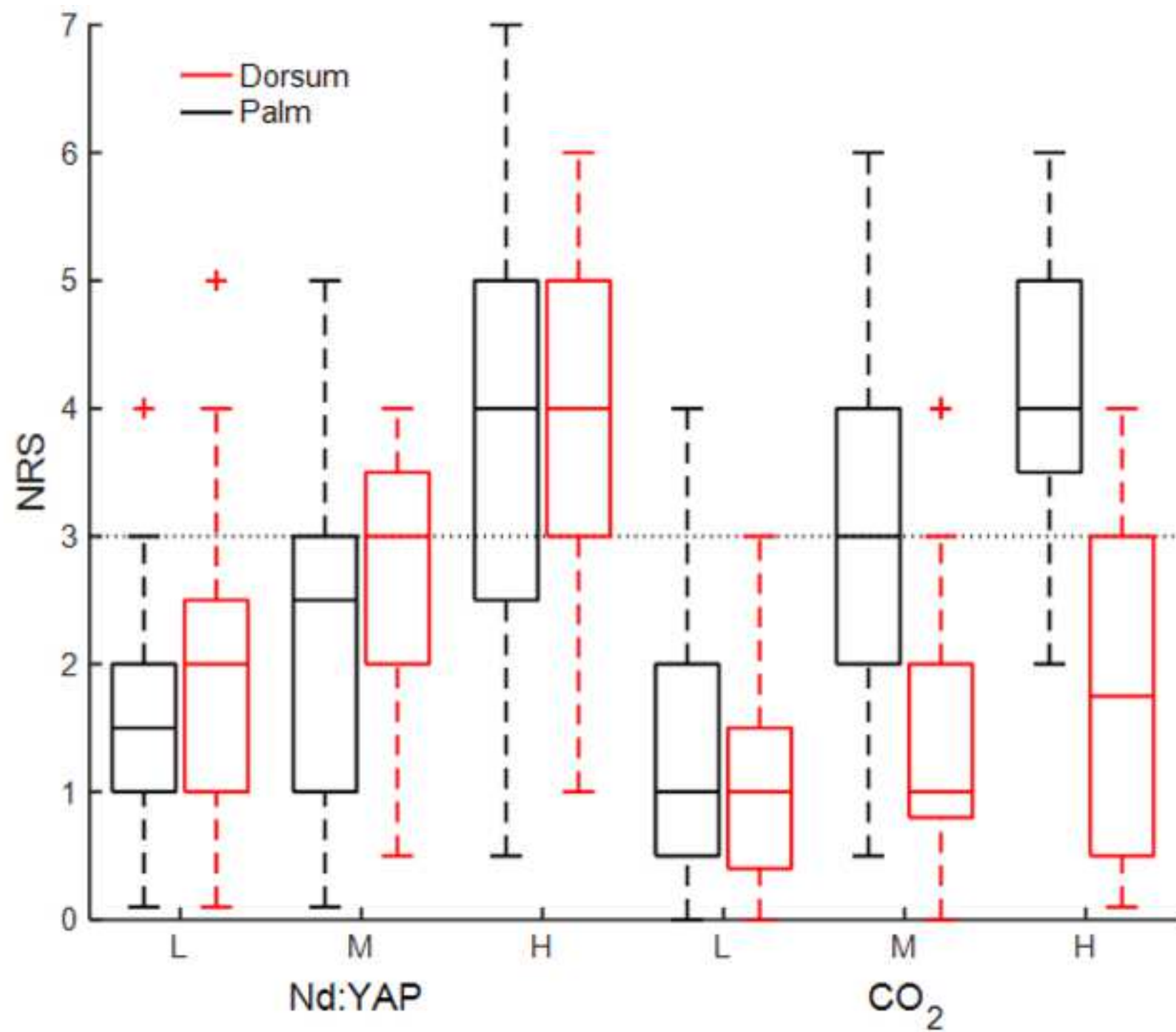
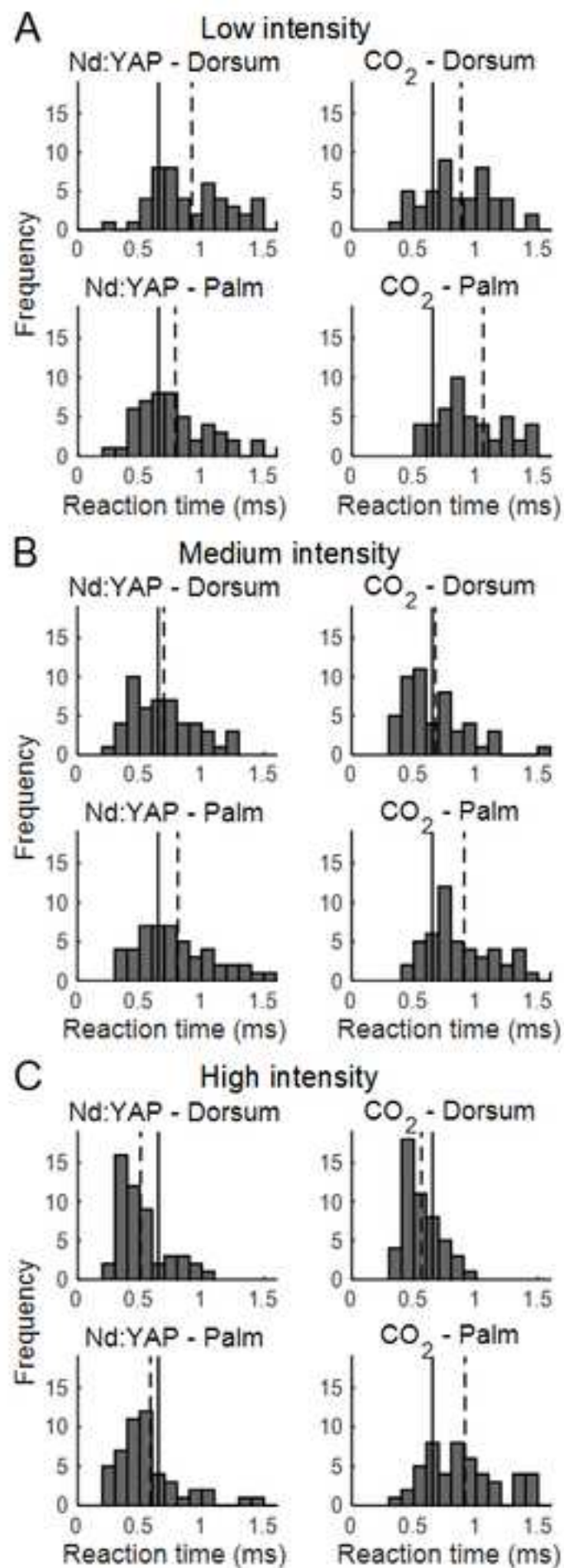
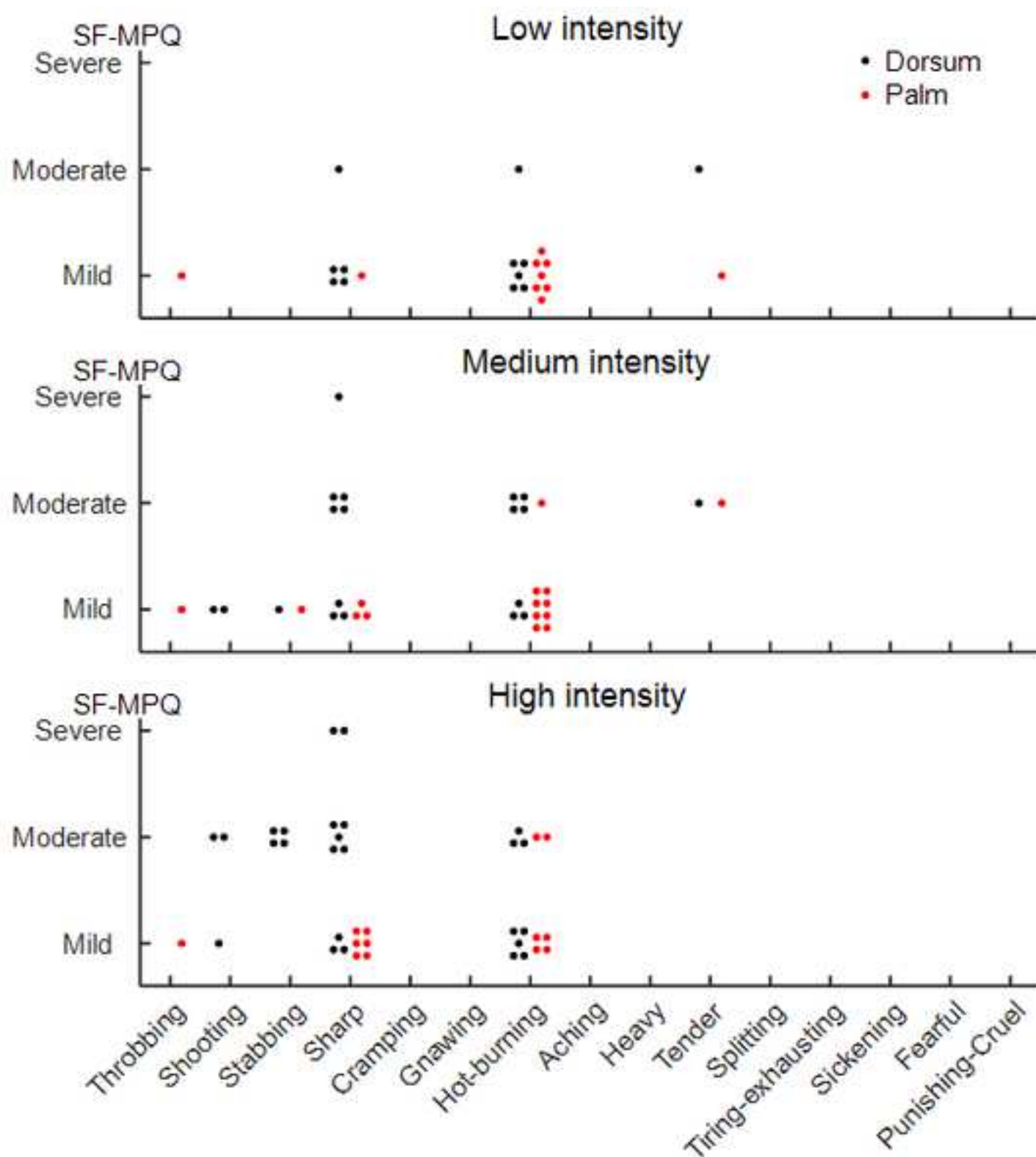
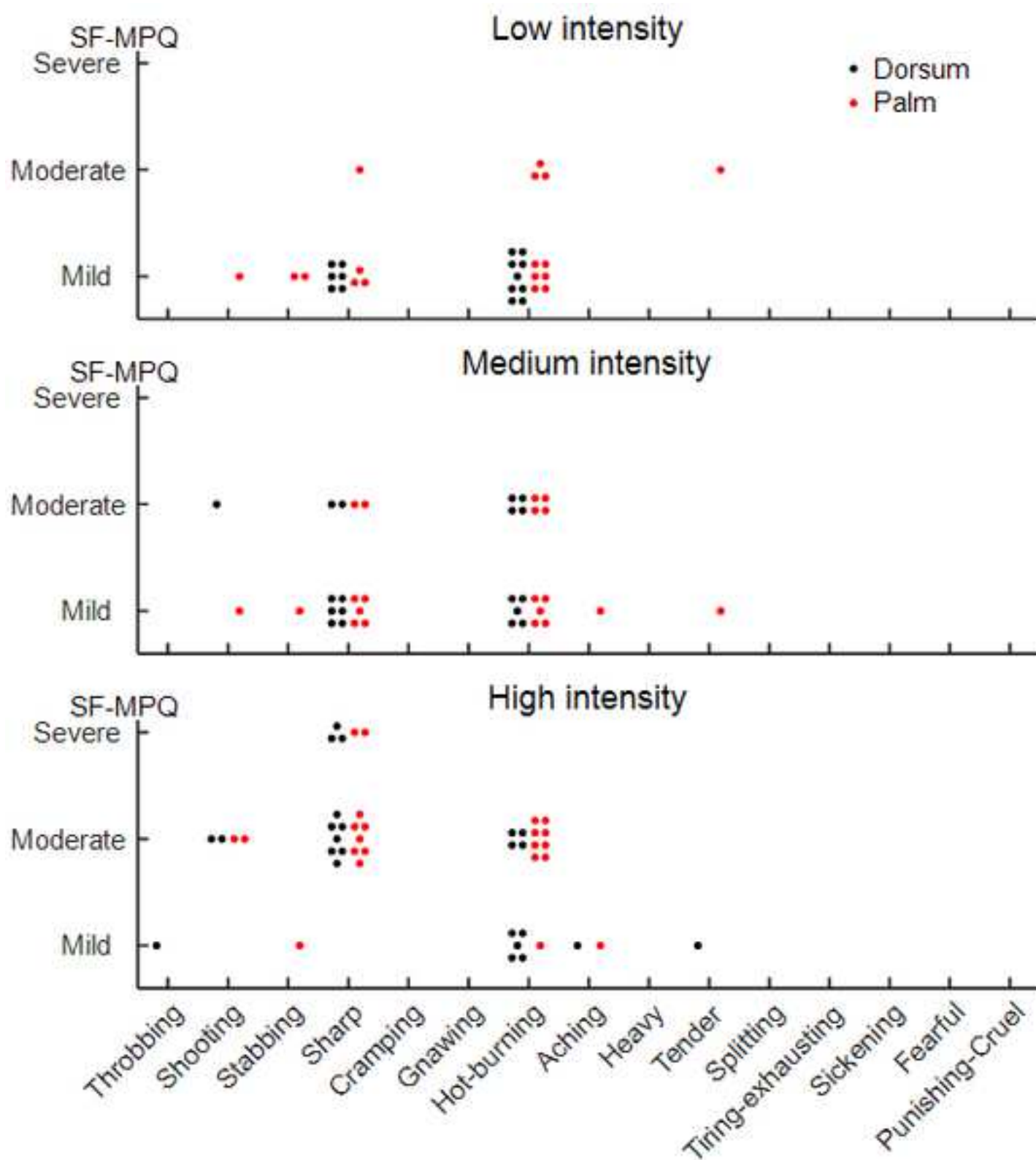


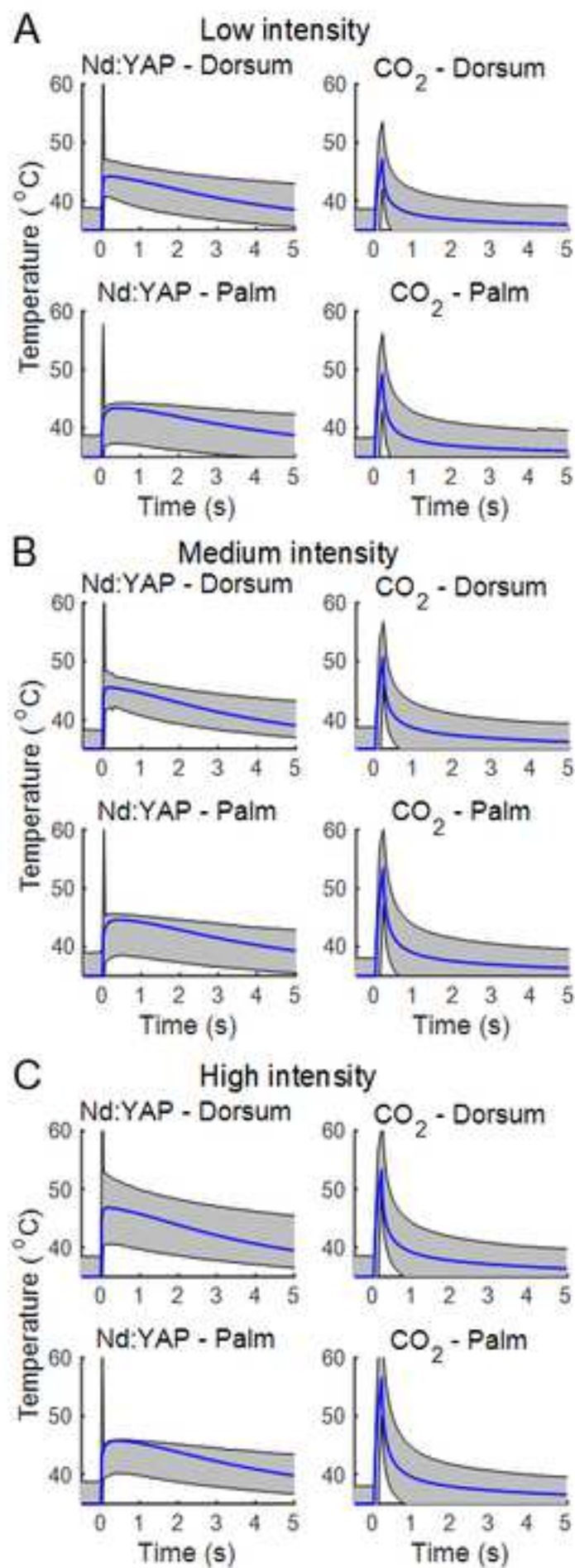
Figure2

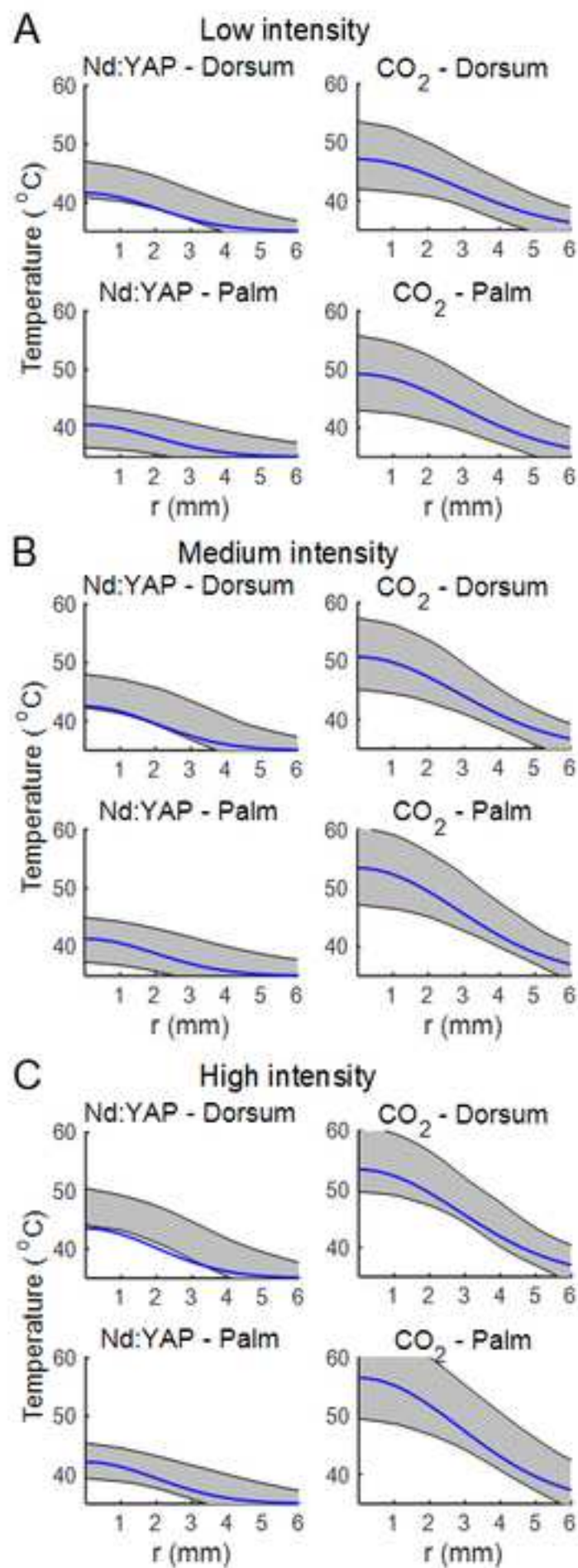


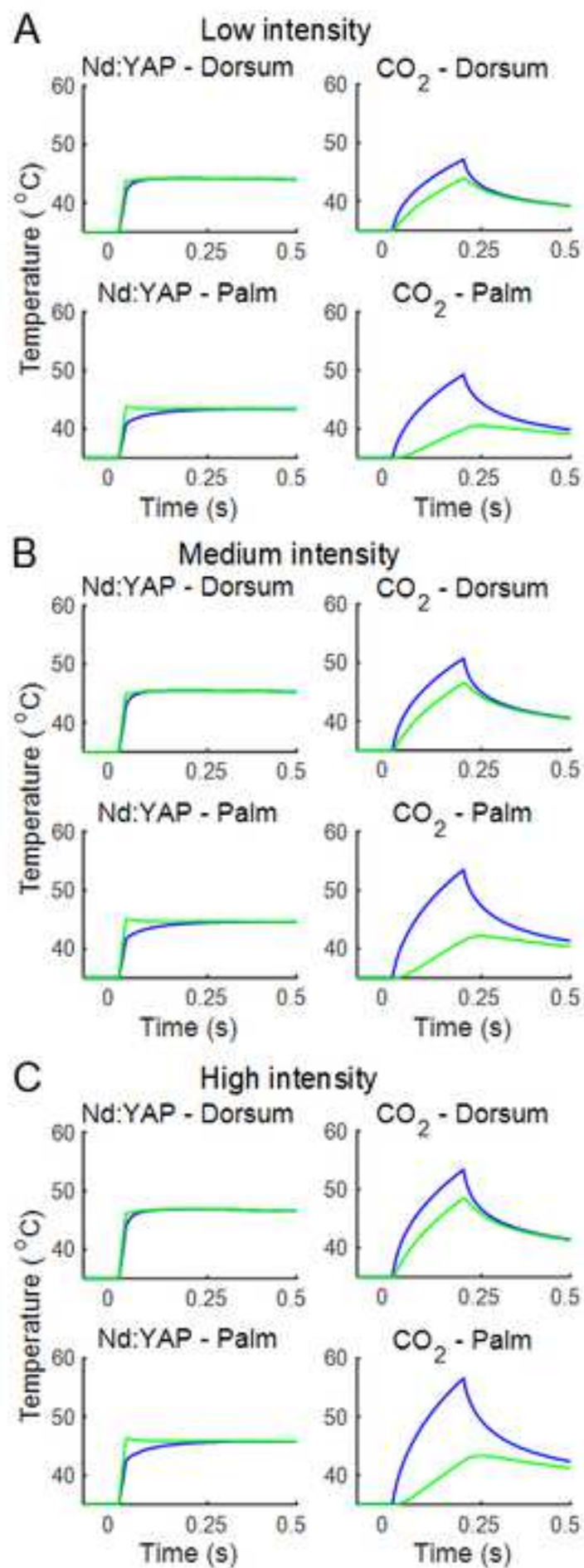


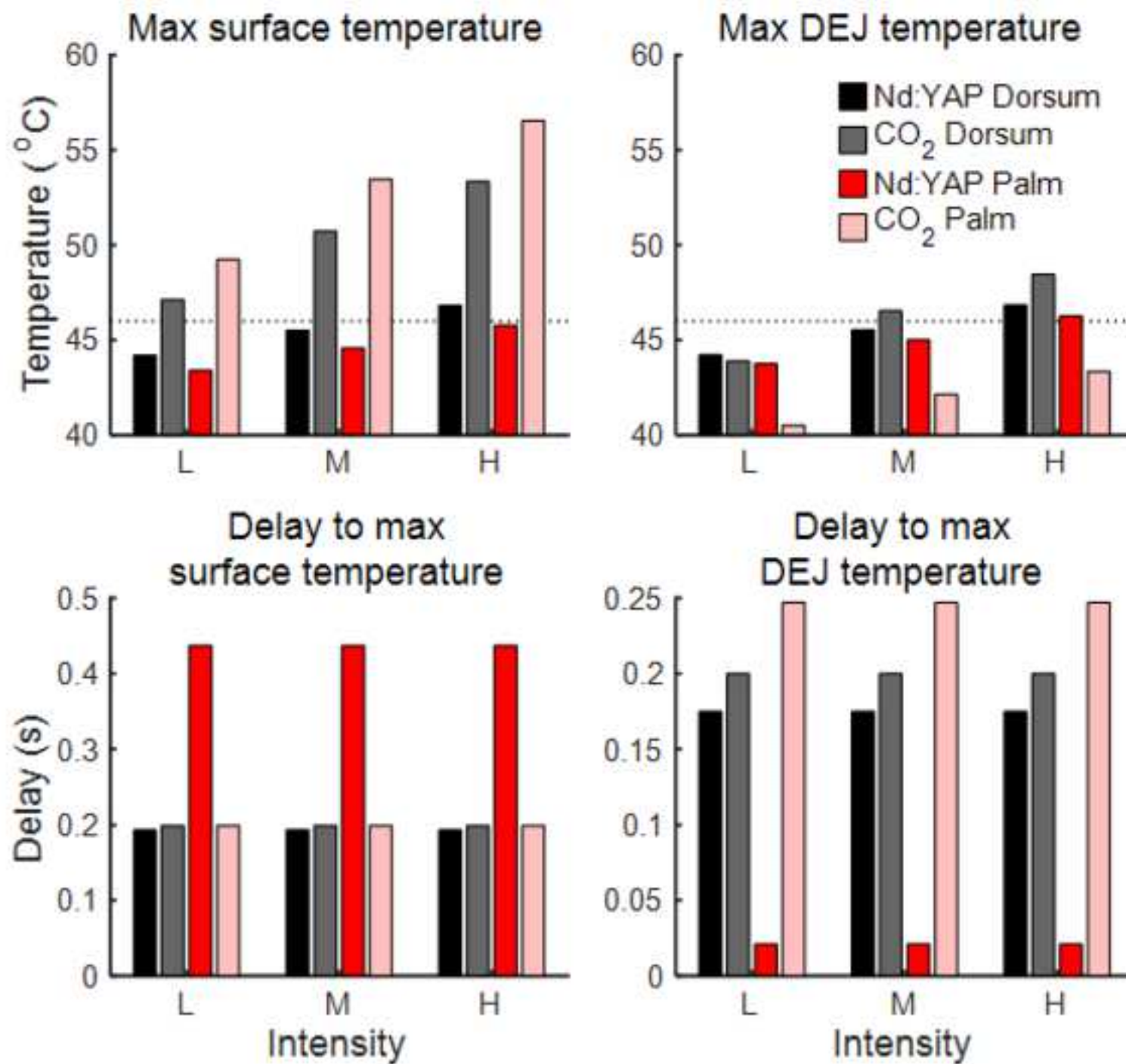


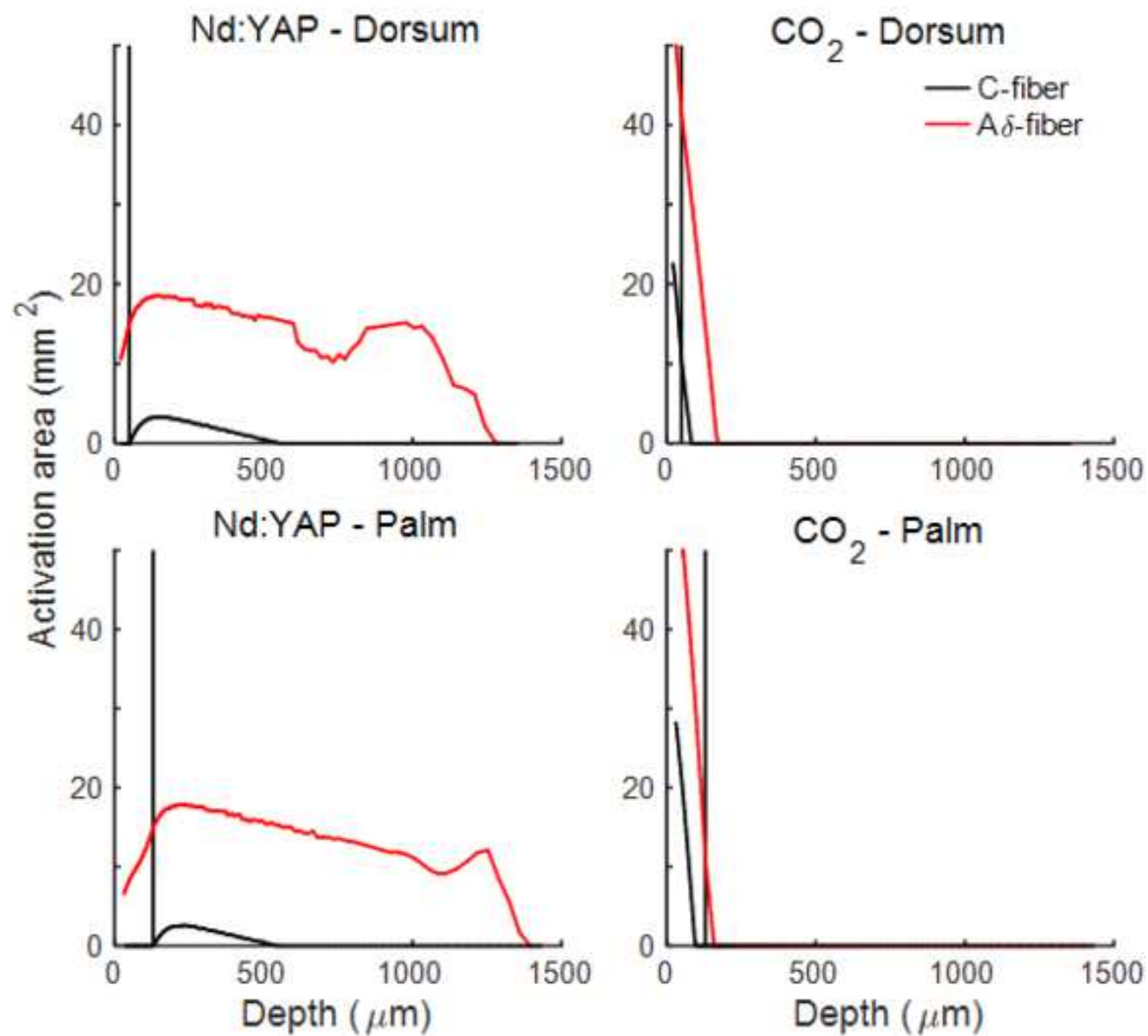


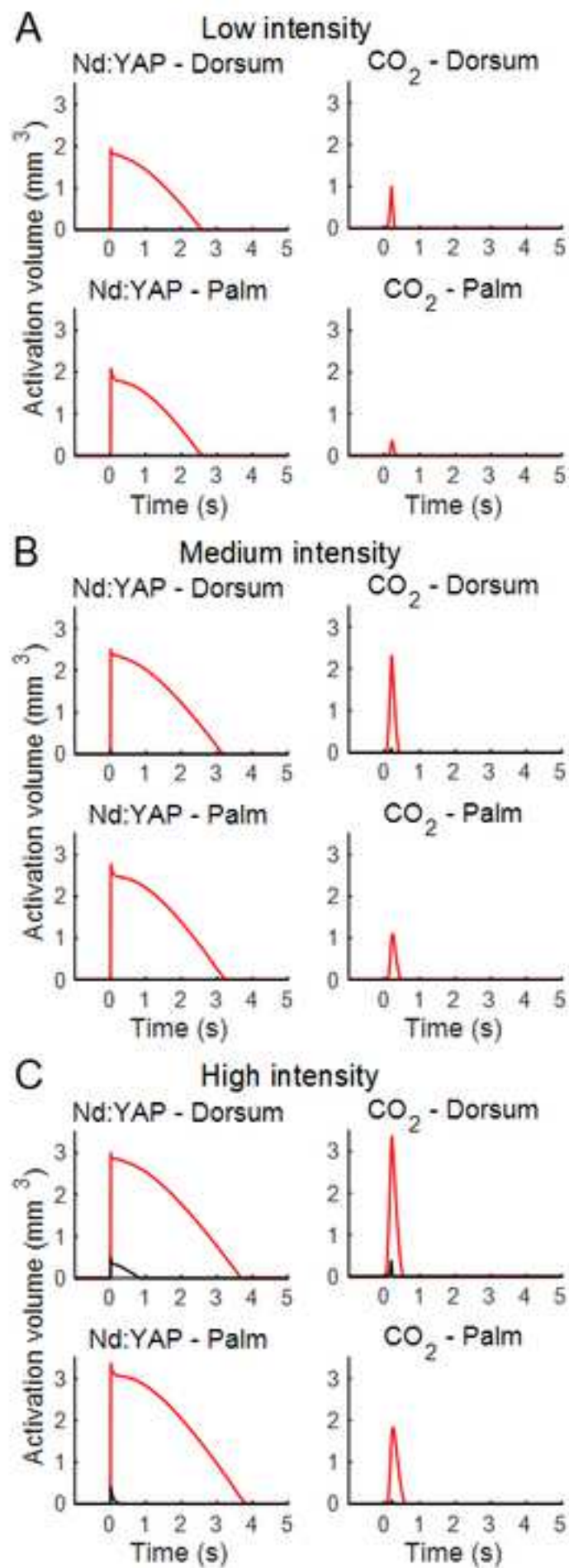


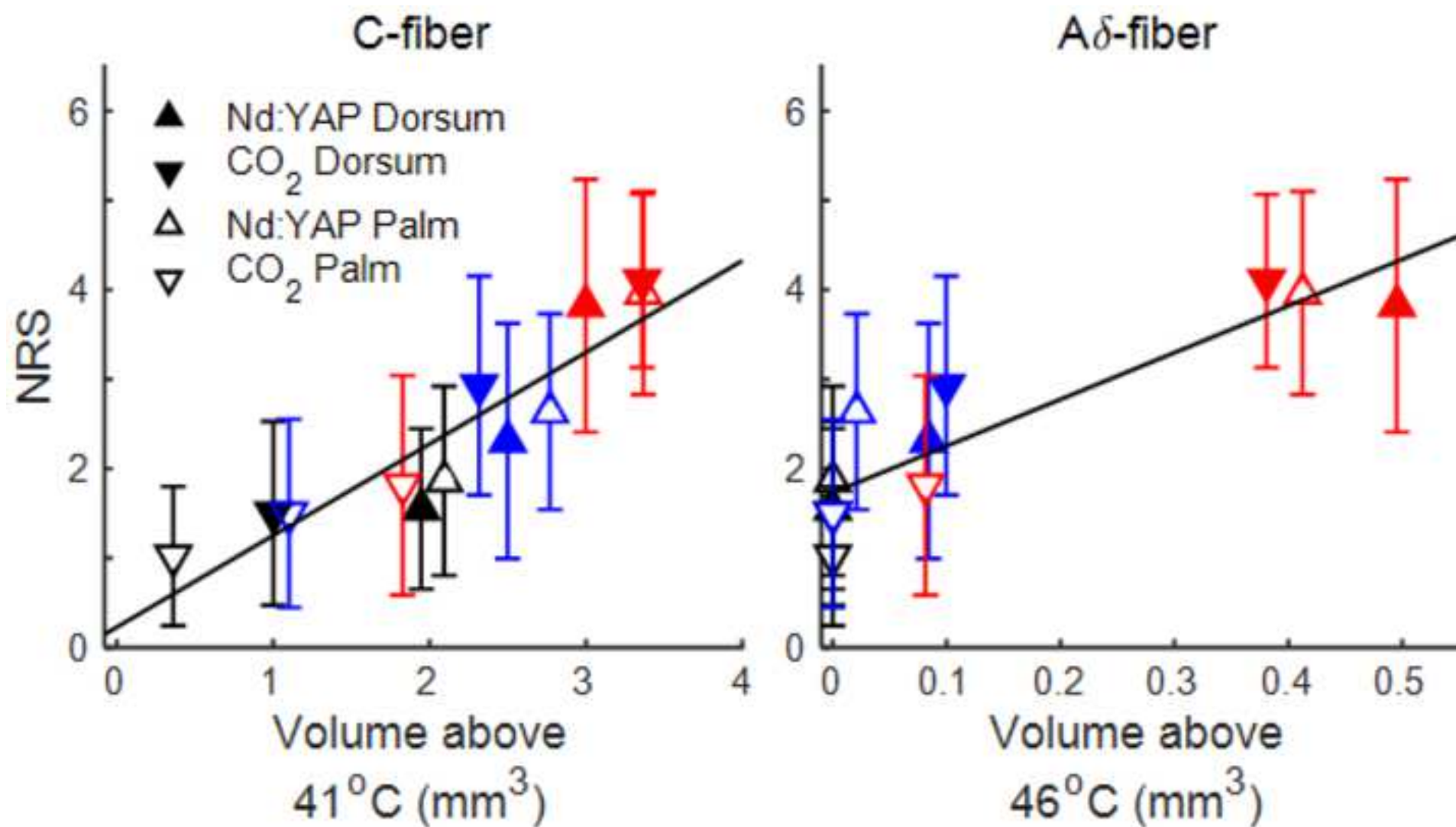












Figures captions R1

Figure 1 – Model geometry including optical and thermal parameters. k : thermal conductivity, c : specific heat, ρ : density, μ_a : absorption coefficient. The model was developed using a 2D-axial symmetry, the symmetry axis is seen to left (dashed line). The thickness of the stratum corneum and vital epidermis was changed according to the type of tissue being modelled (Frahm et al., 2010). The width of the model was 5 cm.

Figure 2 – ~~Boxplot of reported~~ NRS values for different skin and laser types and intensities (L: Low, M: Medium, H: high stimulation intensities). The CO₂ laser stimuli in the palm resulted in significantly lower NRS values (RM-ANOVA, $p < 0.001$). The horizontal dashed line indicate NRS = 3 pain threshold. In each boxplots, the box depicts the 25th and 75th quartiles, the horizontal line in each box depict the median and the error bars depict the 5th and 95th percentile. Outliers are depicted as +.

Figure 3 – ~~Frequency distribution of R~~ reaction times for different skin and laser types and intensities. The vertical full line indicates a 650 ms cut-off value, indicating reaction times associated with A δ fiber responses, longer reaction times indicate C fiber responses. The vertical dashed line indicate the mean for each condition.

Figure 4 – ~~Boxplot of the r~~ Responses to the short-form McGill Pain Questionnaire (SF-MPQ) for the CO₂ laser. For CO₂ laser stimuli, the use of the 'Sharp' descriptor was lower in the palm for CO₂ laser stimuli, suggesting lower activation of A δ fibers. Each point represents the response for a single subject. Non-used responses (i.e. 'None') are not depicted.

~~In each boxplots, the box depicts the 25th and 75th quartiles, the horizontal line in each box depict the median and the errorbars depict the 5th and 95th percentile.~~

Figure 5 – ~~Boxplot of the r~~ Responses to the short-form McGill Pain Questionnaire (SF-MPQ) for the Nd:YAP laser. For Nd:YAP laser stimuli, there were minor differences in the reported descriptors between skin types. Each point represents the response for a single subject. Non-used responses (i.e. 'None') are not depicted.

~~In each boxplots, the box depicts the 25th and 75th quartiles, the horizontal line in each box depict the median and the errorbars depict the 5th and 95th percentile.~~

Figure 6 – Model validation – temporal comparison of model vs. experimental data. The temperature profiles of the model (blue) and the 95 % CI of the experimental IR data (grey area) for the temporal temperature profile at the skin surface. Each subplot (A, B, C) contains the results for three different intensities (Low, medium and high) and for each combination of laser type (Nd:YAP & CO₂) and skin type (dorsum & palm). Generally, the vast majority of the temporal temperature profiles predicted by the model were within the 95 % CI of the experimental IR data.

Figure 7 – Model validation – spatial comparison of model vs. experimental data. The temperature profiles of the model (blue) and the 95 % CI of the experimental IR data (grey area) for the spatial temperature profile at the skin surface. Each subplot (A, B, C) contains the results for three different intensities (Low, medium and high) and for each combination of laser type (Nd:YAP & CO₂) and skin type (dorsum & palm). The spatial profiles were extracted at the time point when the maximum temperature was reached. Generally, the vast majority of the spatial temperature profiles predicted by the model were within the 95 % CI of the experimental IR data.

Figure 8 – Skin surface (blue line) and dermo-epidermal junction (DEJ, green line) temperature profiles over time. For three different stimulation intensities (A, B, C), two different skin types (dorsum & palm) and two

different laser types (Nd:YAP & CO₂) are shown. There was little difference between the surface and the DEJ temperatures for the Nd:YAP laser. On the other hand, there is a clear discrepancy between the skin surface temperature and DEJ for the CO₂ laser, and this difference is exacerbated for stimuli in glabrous skin.

Figure 9 – Maximum simulated surface and dermo-epidermal junction (DEJ) temperatures and delay to reach maximum temperature for each combination of skin, laser types and intensities (L: Low, M: Medium, H: High stimulation intensities). Top row: dashed lines indicate 46 °C, the activation threshold for A δ fibers. Note: the stimulus duration for the Nd:YAP laser was 20ms and for the CO₂ laser it was 200ms.

Figure 10 – Integration of total activated areas at different tissue depths. The figure depicts the areas simulated at stimulus end for the highest stimulation intensity for the Nd:YAP and CO₂ lasers. The red line indicates tissue temperature above C-fiber nociceptor threshold (41°C) and the black line indicates tissue temperature above A δ -fiber nociceptor threshold (46°C). The vertical grey line indicates the dermo-epidermal junction.

Figure 11 – Tissue volume above nociceptor activation threshold over time. Red: 41°C thermal threshold for C-fiber nociceptors, black: 46°C thermal threshold for A δ fiber nociceptor. Each subplot (A, B, C) contains the results for three different intensities (Low, medium and high) and for each combination of laser type (Nd:YAP & CO₂) and skin type (dorsum & palm).

Figure 12 – Comparison between simulated volume above nociceptor threshold (right: C-fiber, 41°C – left: A δ fiber, 46°C) and the experimentally found average NRS values. The colors indicate stimulation intensity (low: black, medium: blue, high: red). For both C and A δ fibers there was a significant correlation (black line) between the stimulated volumes and the NRS ($p < 0.0001$, $r > 0.9$). NRS values are indicated as mean \pm SD.